Available online at www.sciencedirect.com
SCIENCE DIRECT
Planetary and Space Science 54 (2006) 855–870
Planetary and Space Science
www.elsevier.com/locate/pss

Stochastic circumplanetary dynamics of rotating non-spherical dust particles

Martin Makuch[a,*], Nikolai V. Brilliantov[a], Miodrag Sremčević[b], Frank Spahn[a], Alexander V. Krivov[c]

[a]Institute of Physics, University of Potsdam, Am Neuen Palais 10, Bldg. 19, 14469 Potsdam, Germany
[b]Laboratory of Atmospheric and Space Physics, University of Colorado, Boulder, USA
[c]Astrophysical Institute and University Observatory, Friedrich Schiller University, Jena, Germany

Received 22 November 2005; accepted 4 May 2006
Available online 11 July 2006

Abstract

We develop a model of stochastic radiation pressure for rotating non-spherical particles and apply the model to circumplanetary dynamics of dust grains. The stochastic properties of the radiation pressure are related to the ensemble-averaged characteristics of the rotating particles, which are given in terms of the rotational time-correlation function of a grain. We investigate the model analytically and show that an ensemble of particle trajectories demonstrates a diffusion-like behaviour. The analytical results are compared with numerical simulations, performed for the motion of the dusty ejecta from Deimos in orbit around Mars. We find that the theoretical predictions are in a good agreement with the simulation results. The agreement however deteriorates at later time, when the impact of non-linear terms, neglected in the analytic approach, becomes significant. Our results indicate that the stochastic modulation of the radiation pressure can play an important role in the circumplanetary dynamics of dust and may in case of some dusty systems noticeably alter an optical depth.

PACS: 96.30.Gc; 94.10.Nh; 02.50.Ey; 96.30.Wr

Keywords: Mars; Deimos; Ejecta; Stochastics; Radiation pressure

1. Introduction

Dust belts and rings formed by small dust grains orbiting planets are an important component of the solar system. Examples are the E-ring of Saturn, inner dust rings of Jupiter (Burns et al., 1984), tenuous dust rings between the orbits of Jovian satellites Europe, Ganymede and Callisto (Krivov et al., 2002), dust bands of Uranus (Esposito et al., 1991). It is also expected that ejecta from Phobos and Deimos give rise to the dust belts of Mars, whose existence is not yet confirmed (Krivov et al., 2006).

For the dust particles, whose size ranges from approximately 0.01–100 μm, many non-gravitational perturbations, such as direct radiation pressure (e.g. Burns et al., 1979), Lorentz force (Horányi et al., 1991), Poynting–Robertson force (e.g. Makuch et al., 2005) or plasma drag (e.g. Dikarev, 1999) may play a key role in determining their dynamics. Due to the physical nature of these forces they necessarily contain not only an average deterministic component, but also a stochastic component, which may be of different origin. The influence of the stochastic part of the Lorenz force due to the fluctuating magnetic field has been studied in detail by Spahn et al. (2003). Here, we address the stochastic component of the radiation pressure caused by spinning of non-spherical particles. If a non-spherical particle changes its orientation in space, its cross-section with respect to the impinging solar radiation varies accordingly. This causes a variation of the radiation pressure, i.e. a time modulation of the force acting on the particle. For an ensemble of dust particles the modulated force may be represented as a sum of a deterministic mean

*Corresponding author. Tel.: +49 331 9771390; fax: +49 331 9771142.
E-mail address: makuch@agnld.uni-potsdam.de (M. Makuch).

0032-0633/$ - see front matter © 2006 Elsevier Ltd. All rights reserved.
doi:10.1016/j.pss.2006.05.006

force and a fluctuating random force. Knowing the properties of this stochastic force one can analyse how it influences the particle dynamics.

In the present study we develop a model of the stochastic radiation pressure due to the rotational motion of non-spherical grains and analyse its impact on the circumplanetary motion. We elaborate an analytical approach for the general case and perform numerical simulations for the particular case of the circum-Martian dynamics of dust particles. The latter seems to be one of the most promising application of the new approach, since the previous theories, based on the deterministic models failed to explain the negative result of the current attempts to detect the Martian dust tori.

The paper is organized as follows. In Section 2 the general equation of motion is formulated and the necessary notations are introduced. In Section 3 we address the role of particle rotation, formulate the stochastic radiation pressure model, and implement it into the equation of motion. In this section we also present a simplified analytical analysis of the circumplanetary stochastic motion. In Section 4 an extended analytical solution to this problem is given. Section 5 applies the general theory to the circum-Martian dust dynamics. We perform comprehensive numerical investigations and compare the simulation results with the theoretical predictions. In Section 6 we summarize our findings. Some computation details are given in the Appendix.

2. Equation of motion

In order to model the circumplanetary particle dynamics it is necessary to consider a set of different forces. The impact of planetary oblateness, the deterministic part of direct radiation pressure, and Poynting–Robertson drag has been studied in context of circum-Martian motion by Makuch et al. (2005). Here, however, we focus on the stochastic perturbation of the radiation pressure due to rotation of non-spherical particles. Generally, the equation of motion of a dust particle, for the set of perturbations addressed here, may be written as follows:

$$m\ddot{\vec{r}} = -mGM\nabla\left(\frac{1}{r}+\frac{R^2}{r^3}J_2P_2(\vec{r})\right)+BS_r\vec{e}_\odot. \quad (1)$$

The first term on the right-hand side represents the gravity of an oblate planet (e.g. Mars) and the second one direct radiation pressure. Here, r denotes the radius vector of the particle in planetocentric coordinates, M and R mass and equatorial radius of the planet and m is the mass of the dust grain. J_2 is the oblateness coefficient ($J_2 = 1.96\times10^{-3}$ for Mars) and $P_2(\vec{r})$ is the Legendre's polynomial. Factor $B = (Q_{\rm pr}/c)F_\odot(\mathrm{AU}/a_{\rm plan})^2$ characterizes the strength of radiation pressure with the constant $Q_{\rm pr}$ being the radiation pressure efficiency and with the solar energy flux $F_\odot$ at the Earth distance ($F_\odot = 1.36\times10^3\,\mathrm{J\,m^{-2}\,s^{-1}}$) scaled to the distance of the planet $a_{\rm plan}$ by the ratio $(\mathrm{AU}/a_{\rm plan})^2$, c is the speed of light and $S_r = \pi s^2$ the particle cross-section (see e.g. Krivov et al., 1996; Krivov and Jurewicz, 1999). The unit vector $\vec{e}_\odot$ points radially outward from the Sun.

In the numerical analysis of the particle dynamics we directly apply Eq. (1) in its Newtonian form, that is, in the Cartesian coordinates. In this case the Everhart's (1985) method with a constant time step has been employed. A detailed description of the numerical implementation will be given in Section 5.

As shown in the subsequent sections, the perturbation force in Eq. (5) is the stochastic force. Hence the above equation is a stochastic differential equation, which requires a special numerical treatment, discussed in detail in Section 5. In particular, a constant time step is necessary. This significantly reduces the efficiency of the numerical scheme and makes the simulations very time-consuming.

3. Stochastic model for the radiation pressure

3.1. Fluctuations of radiation pressure due to rotation of non-spherical particles

To describe the dynamics of dust grains a simplified assumption about the particles' shape is usually adopted. Particles are assumed to be spheres of radius s with a unique and constant cross-section S_r. However, as it was deduced from the measurements of interplanetary dust, collected in the Earth's stratosphere, "real" grains may be far from being spherical. Particles have a complicated morphology and may be hardly characterized by only one parameter s. Moreover, they continuously spin. Therefore, the particle's cross-section exposed to the solar radiation permanently alters with time. This causes fluctuations of the radiation pressure and thus affects the dynamics of the grains.

To analyse directly the influence of the fluctuating radiation pressure we use equations of motion taking into account a time-dependent particle cross-section $S_r(t)$. Function $S_r(t)$ describes the cross-section. It is obtained by projecting the body boundaries onto a plane perpendicular to the direction of the solar radiation. As already mentioned, the time dependence of the cross-section stems from the non-sphericity of particles and their permanent spinning. Henceforth, we will treat Eq. (1) with time-dependent $S_r(t)$ as an equation, which describes an ensemble of spinning particles with different angular velocities and orientations. This means that we will treat Eq. (1) as a stochastic differential equation. The properties of the stochastic radiation pressure force are determined by the corresponding properties of the fluctuating variable $S_r(t)$. We assume that the rotation of the grains around their centre of mass is not affected by the orbital motion.

Hence we can represent the radiation pressure as a sum of a deterministic part, related to the average cross-section $\langle S_r\rangle$, and a stochastic part fluctuating around its mean according to $\zeta(t) = S_r(t) - \langle S_r\rangle$. Thus, we write the radiation pressure force as

$$\vec{F}_{\rm rp} = F_{\rm rp}\vec{e}_\odot = B\langle S_r\rangle\vec{e}_\odot + B\zeta(t)\vec{e}_\odot, \quad \langle\zeta(t)\rangle = 0. \quad (2)$$

Here we assume that the radiation pressure force acts only in the radial direction defined by $\vec{e}_\odot$ and neglect the contribution of non-radial components. We also assume that the variable $\zeta(t)$ may be treated as a stationary stochastic process with the time-correlation function

$$K(t',t) = \langle \zeta(t)\zeta(t') \rangle = K(|t'-t|) \tag{3}$$

depending on the modulus of the time difference (see e.g. Resibois and de Leener, 1977; Brilliantov and Revokatov, 1996). Physically, $K(t)$ characterizes the memory of the initial orientation of a particle. Naturally, it decays as time grows. This function has a maximum at $t=0$, which, according to the definition of $\zeta(t)$ reads

$$K(0) = \langle \zeta(t)^2 \rangle = \langle S_r^2 \rangle - \langle S_r \rangle^2. \tag{4}$$

With increasing time difference $|t'-t|$, the fluctuations $\zeta(t)$ and $\zeta(t')$ become almost uncorrelated and $K(|t'-t|)$ decays to zero, that is, $K(t\to\infty)=0$. If the rotation frequency of the grains is very fast on the timescale of the orbital motion, the simplest model of δ-correlated white noise may be adopted (Spahn et al., 2003). This already reflects the most prominent properties of the stochastic dynamics.

Since $\zeta(t)$ is determined by the grain orientation, the function $K(t)$ is directly related to the time-correlation function of the particle orientation. Choosing a model of orientational motion, $K(t)$ may be evaluated. The simplest orientation model is a free-rotation model, where the angular momentum of a grain is conserved (Brilliantov and Revokatov, 1996; Pierre and Steele, 1969). A grain can change its angular momentum in several processes—due to collisions with gas atoms or cosmic ray particles, by adsorption/emission of photons, and adsorption/ejection of atoms (Purcell, 1979). The adsorption/emission of photons is related to the Yarkovsky effect (e.g. Spitale and Greenberg, 2001; Skoglov, 2002; Vokrouhlicky and Capek, 2002), while the adsorption/ejection of atoms refers to the so-called photophoresis (e.g. Krauss and Wurm, 2005).

The influence of the direct Yarkovsky effect is negligible, since the temperature gradient, responsible for the effect cannot noticeably develop for quickly rotating and relatively small grains. The reflection/adsorbtion of the solar radiation by the irregular shaped particle may, in principle, cause a random torque (e.g. Vokrouhlicky and Capek, 2002). However, it is expected that this effect could be noticeable only for large and slowly rotating bodies and is negligible for small grains performing a fast rotation. For the typical case of Martian tori, the properties of the near-Martian interplanetary space (Roatsch, 1988) imply that one can neglect collisions with a dilute gas or cosmic rays particles and correspondingly also the effect of photophoresis. We assume that these effects may be also neglected for the other systems addressed in our study. Finally, a torque may arise if a charged grain rotates in a magnetic field (Purcell, 1979). Using the expected angular velocity of grains, $\sim 10^{-1}-10^{3}$ Hz (see the estimates below) and the charge of the particles (Juhász and Horányi, 1995) together with the magnitude of the magnetic field (Juhász and Horányi, 1995), the corresponding torques can be found. Simple estimates then show that particles of the typical size of $\sim 10\,\mu$m subjected to this torque perform a precession with the precession frequency $\sim 10^{-11}-10^{-8}$ Hz when the magnetic field strength corresponds to the Martian or Saturnian environment. Therefore, in what follows we neglect for simplicity this slow precession.

Based on the above analysis we adopt here the free-rotators model for the dust particles. Hence, we treat the system of grains as an ensemble of freely rotating grains with randomly distributed angular momenta. Calculations of the time-correlation function $K(t)$ for this model are rather technical and we therefore present here only the qualitative analysis. Some additional discussion is given in Appendix A.

In order to formulate the model we adopt the following assumptions: First, we assume that particles are symmetric tops with two characteristic lengths, $L_\parallel$, which is parallel to the symmetry axis and $L_\perp$, which is perpendicular to that axis. Second, for an angular velocity distribution of the grains we adopt Gaussian distribution with the characteristic velocity Ω_0 (see Appendix A for more detail). Then the analysis shows that the time-correlation function $K(t)$ depends on time only through the product $\Omega_0 t$, i.e. it may be written as $K(t) = K(0)k(\Omega_0 t)$, where $k(x)$ is a dimensionless function of the dimensionless argument. This result follows also from the dimension reasoning. Third, we consider particles of a simplified form—the figures of rotation. These are obtained by spinning the rectangle of size $2L \times 2l$, with two adjoined semicircles of radius $l<L$ (Fig. 1). Rotating this figure around the axis which passes through its centre and directed along the larger, $2L$-side of the rectangle, yields a *prolate* sphero-cylinder with $L_\parallel = 2L+2l$ and $L_\perp = 2l$. Rotation around the axis that passes through its centre and directed along the shorter $2l$-side yields an *oblate*, disc-shaped particle, with $L_\parallel = 2l$ and $L_\perp = 2L+2l$. Using these models for the particle shapes drastically simplifies the analysis, still reflecting their basic characteristics.

As it will be shown below, the characteristic time of the orbital motion of the dust particles (the orbital period) is much larger than the correlation time of the stochastic variable ζ, estimated as $\sim 1/\Omega_0$. In other words, on the timescale of orbital motion, the grains immediately loose their memory about the previous orientation. Mathematically, this statement formulated as an approximation reads

$$K(t) \simeq 2K_0\delta(t), \tag{5}$$

which holds with a high accuracy. Hence, we approximate the fluctuating variable $\zeta(t)$ by a δ-correlated (white) noise with an amplitude $\sqrt{2K_0}$. The constant K_0 may be derived from the relation

$$\begin{aligned} K_0 &= \int_0^\infty K(t)\,\mathrm{d}t = K(0)\int_0^\infty k(\Omega_0 t)\,\mathrm{d}t \\ &= K(0)\Omega_0^{-1}A = K(0)\left(\frac{\Omega_0}{A}\right)^{-1}, \end{aligned} \tag{6}$$

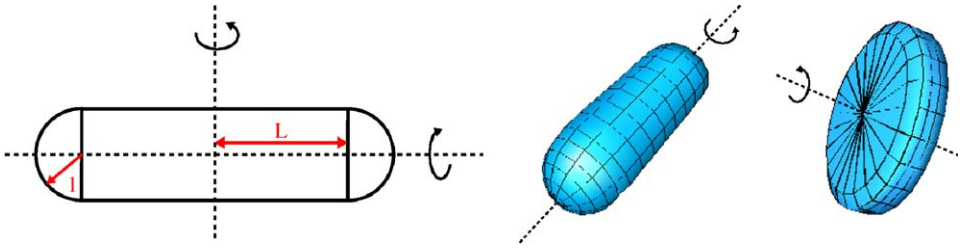

Fig. 1. The particles are assumed to be figures of rotation: middle—prolate particles with $L_{\parallel} = 2L + 2l$ and $L_{\perp} = 2l$, right—oblate particles, with $L_{\parallel} = 2l$ and $L_{\perp} = 2L + 2l$. In both cases, the aspect ratio is equal to $\alpha = L/l$.

where the property of the δ-function and the definition of the dimensionless function k is used. As it is shown in Appendix A, the constant A in Eq. (6) is of the order of unity. Since the rotation frequency Ω_0 is not experimentally known and may be estimated only with a large uncertainty, it suffices to apply the simplifying assumption, $A = 1$. Alternatively, the parameter Ω_0 in what follows may be treated as the ratio Ω_0/A, since as it is seen from Eq. (6), the value of K_0 depends only on this ratio.

With the above assumptions we arrive at the following stochastic model for the radiation pressure force:

$$\vec{F}_{\rm rp} = F_{\rm rp}\vec{e}_{\odot} = B\langle S_r\rangle\vec{e}_{\odot} + B\sqrt{2K_0}\,\xi(t)\vec{e}_{\odot}, \tag{7}$$

where $\xi(t)$ denotes white noise with zero mean and unit dispersion

$$\langle\xi(t)\rangle = 0, \quad \langle\xi(t_1)\xi(t_2)\rangle = \delta(t_1 - t_2). \tag{8}$$

In order to proceed either analytically or numerically we need to find the quantities K_0 and Ω_0, which will be done in next section.

3.2. Basic parameters of the grain's orientational time-correlation function

3.2.1. Amplitude of the time-correlation function

For *prolate* particles the projection area on the plane perpendicular to the solar radiation depends on the angle $\theta(t)$ between the symmetry axis of a particle and the direction of the radiation as

$$S_r(t) = 4Ll\sin\theta(t) + \pi l^2, \tag{9}$$

so that the mean-square average value of this quantity reads,

$$\langle S_r(t)^2\rangle = 16L^2l^2\langle\sin^2\theta(t)\rangle + 8\pi Ll^3\langle\sin\theta(t)\rangle + \pi^2l^4. \tag{10}$$

For free rotators, the distribution of the particle axes in space is assumed to be spherically symmetric, giving

$$\langle\sin\theta(t)\rangle = \frac{\pi}{4}, \quad \langle\sin^2\theta(t)\rangle = \frac{2}{3}, \tag{11}$$

and finally

$$K(0) = \langle S_r^2\rangle - \langle S_r\rangle^2 = L^2l^2(\tfrac{32}{3} - \pi^2) = 0.7971L^2l^2. \tag{12}$$

For *oblate* particles similar calculations may be performed. Introducing the aspect ratio, $\alpha = L/l + 1$, as the ratio of maximal to minimal size of the particle, we write the expressions for K_0 and $\langle S_r\rangle$ for both types of particles in a compact form

$$\langle S_r\rangle = \pi l^2\begin{cases}\alpha & \text{prolate particles,}\\ \dfrac{\alpha(\alpha+1)}{2} & \text{oblate particles,}\end{cases} \tag{13}$$

and

$$K_0 = l^4\Omega_0^{-1}\begin{cases}0.7971(\alpha-1)^2 & \text{prolate particles,}\\ 0.8224\alpha^2(\alpha-1)^2 & \text{oblate particles.}\end{cases} \tag{14}$$

3.2.2. Characteristic rotation frequency

We assume that the system of dust particles is very rarified, so that the collisions between grains or collisions of the grains with other particles, such as gas molecules, ions, etc. are extremely rare and cannot support any "thermal" distribution of the angular velocity in an ensemble of rotating grains. Hence the rotation frequency of the grains is determined by the mechanisms of their creation. There could be several mechanisms, among which the impact-ejecta one is the most important.

According to the presently accepted theoretical model of the impact-ejecta process, the hypervelocity impacts of interplanetary dust particles cause an ejection of secondary material. The total mass of ejected grains is several orders of magnitude higher than the mass of impactors. The velocities of ejecta are of the order of, or higher than, the escape velocity of the parent bodies (approximately $1-10\,\mathrm{m/s}$). The tiny grains which successfully leave the action sphere of the parent bodies finally create dust complexes surrounding the bodies or their orbits.

When a fast particle (micrometeoroid) collides with a surface of a satellite it creates a crater on the surface of diameter $D_{\rm crat}$. All the material of the surface initially located in the crater is crashed into small pieces which are ejected into space with the characteristic velocity $v_{\rm ej}$. Estimates of the angular velocity of the ejected particles may be performed for the case of a rocky surface (Brilliantov et al., 2006), which yields the following result:

$$\Omega_0 \sim \frac{v_{\rm ej}}{D_{\rm crat}}. \tag{15}$$

Using $v_{\rm ej} = 5\,\mathrm{m/s}$ for a typical ejection velocity and $D_{\rm crat} = 20\times10^{-4}\,\mathrm{m}$, for a typical crater diameter we

estimate the characteristic frequency as $\Omega_0 \approx 5 \times 10^3\,\mathrm{s}^{-1}$. The corresponding timescale of the rotation motion, ($\Omega_0^{-1} \approx 10^{-3}$ s) is much smaller than the orbital timescale which is of the order of $\sim 10^5$ s, if one uses the ejection from Deimos as an example. This justifies the application of the simple model of δ-correlated white noise.

Another possible mechanism of particle creation may be the eruption of dust due to volcanic (or cryovolcanic) activity at some celestial bodies. One can mention the Jupiter satellite Io as an example. The eruption of dust is accompanied by that of a gas (sulphur, in the case of Io). One can assume that during the eruption the dust grains are in a transient thermal equilibrium with the gas. They decouple however from the gas after escaping from the body into space. In this case the angular velocity of the grains is determined by the temperature of the gas:

$$\Omega_0 \sim \sqrt{\frac{k_\mathrm{B} T}{I}}, \tag{16}$$

where k_B is the Boltzmann constant, T is the temperature of the gas and I is the characteristic moment of inertia of a grain. Assuming that the temperature of the gas ranges from 10^2 to 10^3 K (the temperature in the eruption zone of Io is estimated as 1800 K) we obtain that Ω_0 varies in the interval 1–4 Hz for particles of size $\sim 10\,\mu$m and density $2.37 \times 10^3\,\mathrm{kg/m^3}$. This value of the angular velocity satisfies the requirement of fast rotation, which makes the application of the white noise model valid.

3.3. Role of stochasticity in the dust dynamics: simplified analysis

Before starting comprehensive analytical or numerical study of the impact of the stochastic radiation pressure on the circumplanetary dynamics, it is worth to perform simplified analysis, choosing a simple model.

Consider a particle moving around a planet on a circular orbit with zero inclination. The perturbation equation for the semimajor axis a reads (e.g. Burns, 1976):

$$\frac{\mathrm{d}a}{\mathrm{d}t} = \frac{2a^2}{GM}\frac{\dot{E}}{m}. \tag{17}$$

Here the constants G, m and M have been defined previously, and $\dot{E}$ denotes the rate of change of the particle energy due to the perturbation of the radiation pressure force. Using Eq. (2) we write

$$\dot{E} = \vec{F}_\mathrm{rp} \cdot \vec{v} = F_\mathrm{rp}(\vec{v} \cdot \vec{e}_\odot), \tag{18}$$

where $\vec{v}$ is the velocity of the particle, which is on the circular orbit constant. That is $v = na$, with $n = \sqrt{MG/a^3}$ being the mean orbital motion of the particle. Moreover, choosing the direction to the Sun, $\vec{e}_\odot$ along the x-axis, we write

$$\vec{v} \cdot \vec{e}_\odot = v_x = -v \sin nt = -na \sin nt. \tag{19}$$

Hence, we obtain,

$$\frac{\mathrm{d}a}{\mathrm{d}t} = -\frac{2}{mn^2 a} F_\mathrm{rp} na \sin nt \simeq -\frac{2}{mn_0} F_\mathrm{rp} \sin n_0 t, \tag{20}$$

where in the last equation we for simplicity approximate the mean motion n by its initial value n_0. The solution to Eq. (20) may be written as

$$a(t) = a_0 - \int_0^t \frac{2}{mn_0} F_\mathrm{rp}(t') \sin n_0 t'\,\mathrm{d}t', \tag{21}$$

where a_0 is the initial value of the semimajor axis and $F_\mathrm{rp}(t)$ depends on time via the stochastic component $B\sqrt{2K_0}\xi(t)$, see Eq. (2). The ensemble average of a then reads

$$\langle a \rangle = a_0 - \int_0^t \frac{2}{mn_0} \langle F_\mathrm{rp}(t') \rangle \sin n_0 t', \tag{22}$$

which implies the following time-dependent fluctuation of this orbital element:

$$\begin{aligned} \delta a(t) = a(t) - \langle a \rangle &= -\int_0^t \frac{2}{mn_0} [F_\mathrm{rp} - \langle F_\mathrm{rp} \rangle] \sin n_0 t'\,\mathrm{d}t' \\ &= -\int_0^t \frac{2}{mn_0} B\sqrt{2K_0}\xi(t') \sin n_0 t'\,\mathrm{d}t'. \end{aligned} \tag{23}$$

In Eq. (23) we use (2) and take into account that $\langle F_\mathrm{rp} \rangle = B\langle S_r \rangle$. Correspondingly, the reduced standard deviation of the element depends on time as

$$\begin{aligned} \frac{\langle (\delta a)^2 \rangle}{a_0^2} &= \frac{8B^2K_0}{m^2 n_0^2 a_0^2} \int_0^t \mathrm{d}t' \int_0^t \mathrm{d}t'' \langle \xi(t')\xi(t'') \rangle \sin n_0 t' \sin n_0 t'' \\ &= \frac{8B^2K_0}{m^2 n_0^2 a_0^2} \int_0^t \sin^2 n_0 t'\,\mathrm{d}t' \\ &= \frac{4B^2K_0}{m^2 n_0^2 a_0^2} \left(t + \frac{1}{2n_0} \cos 2n_0 t \right), \end{aligned} \tag{24}$$

where we take into account the property of the white noise, $\langle \xi(t')\xi(t'') \rangle = \delta(t' - t'')$. For the time addressed here, $n_0 t \gg 1$, which corresponds to many rotation periods of the particle around the planet, one can neglect the oscillating terms in the last equation, which yields the diffusion-like equation for the standard deviation,

$$\frac{\langle (\delta a)^2 \rangle}{a_0^2} = Dt \tag{25}$$

with the effective "diffusion coefficient"

$$\begin{aligned} D &= \frac{4B^2K_0}{m^2 n_0^2 a_0^2} \\ &= \frac{4B^2 l^4}{m^2 \Omega_0} \frac{a_0}{GM} \begin{cases} 0.7971(\alpha - 1)^2 & \text{prolate particles,} \\ 0.8224\alpha^2(\alpha - 1)^2 & \text{oblate particles,} \end{cases} \end{aligned} \tag{26}$$

where Eq. (14) for K_0 has been used. As it follows from Eqs. (25) and (26) the standard deviation of the semimajor axis for an ensemble of particles grows with time. The rate of its growth strongly depends on the particle's size l and the aspect ratio α. It is also interesting to note that D depends inversely on the average

rotation frequency Ω_0, that is, the diffusion coefficient is smaller if particles rotate fast. Another important feature of the above relation is the dependence on the semimajor axis a_0 and the planet mass M. For particles orbiting around a light planet (small M) on an extended orbit (large a_0) the diffusion coefficient may be very large.

Let us make some estimates for this quantity for an oblate grain orbiting Mars on the Deimos or Phobos orbit. For better comparison with previous studies we define an effective radius ($s_{\rm eff}$) of spherical grain with the cross-section equal to $\langle S_r\rangle$ of an *oblate* particle. Denoting the minimal particle radius l as $s_{\min}$ we obtain the relation $s_{\rm eff}=s_{\min}\sqrt{\alpha(\alpha+1)/2}$. Correspondingly the mass of a particle is $m=\rho_g\pi s_{\min}^3(2\alpha^2+\pi\alpha)$, where $\rho_g=2.37\times 10^3\,{\rm kg/m^3}$ is the bulk density of the grain. For the aspect ratio of particles we choose $\alpha=5$ and the radiation pressure efficiency $Q_{\rm pr}$ is calculated in the same manner as described in Section 5.

Referring for the discussion of the astrophysical relevance to Section 5, we obtain for a grain with $s_{\rm eff}=0.5\,\mu{\rm m}$ rotating with the angular velocity 0.01 Hz the diffusion coefficient $D=3.31\times 10^{-11}\,{\rm s^{-1}}$ for Deimos ejecta and $D=1.32\times 10^{-11}\,{\rm s^{-1}}$ for Phobos one. With this diffusion coefficient the standard deviation of the semi-major axis increases up to 14% of its initial value during 10 Martian years (8.8% for Phobos). For astrophysically more relevant time interval corresponding to mean particle lifetime of one Martian year we get change of 4.4% (2.8% for Phobos). Similarly, for particles with size $s_{\rm eff}=10\,\mu{\rm m}$ rotating with the same frequency from the longest-living Martian population, the diffusion coefficient is $D=1.99\times 10^{-14}\,{\rm s^{-1}}$. This corresponds to the increase of the standard deviation up to 11% during 10 000 Martian years.

The more rigorous analysis given in Section 4 yields essentially the same order-of-magnitude values for the diffusion coefficient.[1]

4. Analytical solution for the stochastic equation of motion

The goal of this section is to analytically estimate effects of the stochastic radiation pressure using linear analysis of the perturbation equations. To this aim we will first introduce a non-singular orbital elements and dimensionless parameters that characterize the strength of radiation pressure and oblateness. Then we proceed calculating the distribution functions, mean and variances of eccentricity, inclination and semimajor axis of ejected particles. The employed calculations are rather technical, and an example of calculations for the case of eccentricity is presented in Appendix B.

[1]In Section 4 we use the dimensionless time $\lambda=n_\odot t$, where $n_\odot$ is the mean motion of the planet, and, respectively, the dimensionless diffusion coefficient Λ. Hence, the diffusion coefficient D of Section 3 is to be compared with $\Lambda n_\odot$.

4.1. Orbital elements and force parameters

Following Krivov et al. (1996), we introduce the non-singular orbital elements

$$h=e\cos\tilde\omega,\quad k=e\sin\tilde\omega,\quad p=\sin i\cos\Omega,\quad q=\sin i\sin\Omega, \tag{27}$$

where $\tilde\omega\equiv\Omega+g$ is the longitude of pericentre and e,i,Ω, and g are eccentricity, inclination, longitude of the node, and the argument of the pericentre, respectively (see Appendix B). As an independent variable, we use the longitude of the Sun λ leading to dimensionless equations of motion. Neglecting the eccentricity of the planet orbit, λ is a linear function of time

$$\lambda=\lambda_{\odot 0}+n_\odot t,\quad n_\odot=\sqrt{GM_\odot/a_{\rm plan}^3}, \tag{28}$$

where $n_\odot$ is the mean motion of the planet and $\lambda_{\odot 0}$ is the initial solar longitude at the moment of ejection ($t_0=0$).

For the further analysis it is convenient to introduce dimensionless force parameters. The radiation pressure is expressed with the coefficient C as (Krivov et al., 1996)

$$C(\lambda)\equiv\frac{3}{2}\frac{F_{\rm rp}}{mn_\odot n_0 a_0}=C_{\rm d}+C_\xi(\lambda), \tag{29}$$

where the radiation pressure force $F_{\rm rp}$ has been defined in Eq. (2) and n_0 denotes the initial mean motion of the grain $n_0^2=GM/a_0^3$. $C_{\rm d}$ is the deterministic component of C and C_ξ is the fluctuating part, modelled as a Gaussian white noise

$$\langle C_\xi(\lambda)\rangle=0,\quad \langle C_\xi(\lambda_1)C_\xi(\lambda_2)\rangle=\sigma^2\delta(\lambda_1-\lambda_2). \tag{30}$$

Taking Eq. (7) into account for the stochastic radiation pressure and comparing it with Eq. (29) we express $C_{\rm d}$ and σ^2 as

$$C_{\rm d}=\frac{3}{2}\frac{B\langle S_r\rangle}{mn_\odot n_0 a_0},\quad \sigma^2=\frac{2C_{\rm d}^2K_0n_\odot}{\langle S_r\rangle^2}, \tag{31}$$

where Eqs. (8) and (30) have been used. The quantities defined in Eq. (31) make a direct link to the terms defined in the previous section.

In what follows we will denote the complete solution for a variable X (X is a certain orbital element) as $X_{\rm t}$, while X_ξ denotes the solution with $C_{\rm d}=0$ and $X_{\rm d}$ the purely deterministic solution with $C_\xi=0$. Correspondingly, for the derivatives with respect to the dimensionless time λ we will use the notation ${\rm d}X/{\rm d}\lambda\equiv X'$.

4.2. General solution for eccentricity

Although the general equations of the motion for the orbital elements are coupled (see Appendix B), it has been demonstrated by Krivov et al. (1996) that for eccentricity components k and h much simpler equations may be obtained. Namely, it is sufficient to consider only the first-order terms in the orbit averaged equations and to ignore inclination components p and q which are significantly

smaller (cf. Eq. (39) in Krivov et al., 1996),

$$h' = -C\cos\varepsilon\sin\lambda - k\omega, \quad k' = +C\cos\lambda + h\omega, \tag{32}$$

where ε is the obliquity of a planet ($\varepsilon = 25^\circ$ for Mars). In general, one needs to consider the full Gauss perturbation equations (e.g. Burns, 1976), since the orbit averaging procedure might disregard certain terms which can give rise to a noticeable diffusion, as it will be demonstrated for the semimajor axis and inclination. However, the presented Eqs. (32) contain the zeroth-order term which is sufficient to explain diffusion of h and k.

The solution $h_\mathrm{d}(\lambda)$ and $k_\mathrm{d}(\lambda)$ to the system (32) for the deterministic case, $C = C_\mathrm{d}$, is known (see Krivov et al., 1996). Eqs. (32) for the purely stochastic case $C = C_\xi$, may be solved with the same reasoning as for the previously given simplified analysis (see Appendix B for detail). The solutions are the normally distributed elements h_t and k_t with mean

$$\langle h_\mathrm{t}(\lambda)\rangle = h_\mathrm{d}(\lambda), \quad \langle k_\mathrm{t}(\lambda)\rangle = k_\mathrm{d}(\lambda), \tag{33}$$

and variance

$$\langle h_\mathrm{t}^2(\lambda)\rangle - \langle h_\mathrm{t}(\lambda)\rangle^2 \approx \langle k_\mathrm{t}^2(\lambda)\rangle - \langle k_\mathrm{t}(\lambda)\rangle^2 \approx \Lambda\lambda, \tag{34}$$

$$\Lambda = \tfrac{1}{8}\sigma^2[3 + \cos(2\varepsilon)]. \tag{35}$$

The resulting eccentricity $e_\mathrm{t} = (h_\mathrm{t}^2 + k_\mathrm{t}^2)^{1/2}$ is not normally distributed. Its mean is

$$\langle e_\mathrm{t}(\lambda)\rangle \approx \sqrt{e_\mathrm{d}^2(\lambda) + \alpha_e\Lambda\lambda}, \tag{36}$$

and the variance reads for the limiting cases of strong and weak noise:

$$\langle e_\mathrm{t}^2(\lambda)\rangle - \langle e_\mathrm{t}(\lambda)\rangle^2 \approx (2 - \alpha_e)\Lambda\lambda, \tag{37}$$

$$\alpha_e = \begin{cases} 1/2, & \Lambda\lambda \ll e_\mathrm{d}^2, \\ \pi/2, & \Lambda\lambda \gg e_\mathrm{d}^2. \end{cases} \tag{38}$$

As it is clearly seen from Eq. (37), the standard deviation of the eccentricity linearly increases with the dimensionless time λ. In other words, the evolution of this orbital element for an ensemble of grain demonstrates the diffusional behaviour.

4.3. Solution for the semimajor axis

In addition to the simplified analysis of Section 3 we wish to present here the corresponding rigorous analysis of the semimajor axis evolution. First, we note that although it remains constant $a_\mathrm{d}(\lambda) \approx a_0$ in the purely deterministic case without the Poynting–Robertson force, this does not hold if an additional stochastic component is present. Unfortunately, in this case it is not possible to use the orbit-averaged equations, but the full perturbation equation for the semimajor axis has to be studied (e.g. Burns, 1976)

$$\frac{\mathrm{d}a}{\mathrm{d}t} = \frac{2}{an^2}\frac{F_\mathrm{rp}}{m}\vec{v}\cdot\vec{e}_\odot, \quad n^2 = \frac{GM}{a^3}, \tag{39}$$

where, as previously, $\vec{v}$ is the particle's velocity and n is the mean motion of the particle. In Eq. (39) we ignored the oblateness of the planet, assuming $\omega \approx 0$, since both the deterministic solution $a_\mathrm{d}(\lambda)$ and moments of h_ξ and k_ξ, as well as p_ξ and q_ξ, are not very sensitive to ω.

Calculating $\vec{v}\cdot\vec{e}_\odot$ and expanding the result around $e_0, i_0 = 0$ we obtain

$$\begin{aligned}\vec{v}\cdot\vec{e}_\odot = & -an[\cos\varepsilon\sin\lambda\cos(\tilde{\omega}+\theta) \\ & - \cos\lambda\sin(\tilde{\omega}+\theta)] + \mathrm{O}(e) + \mathrm{O}(i),\end{aligned} \tag{40}$$

where θ is the true anomaly. Clearly, in the purely deterministic case the orbit average of this equation yields zero. Starting from Eq. (39), introducing the scaled semimajor axis $\tilde{a} = a/a_0$, dimensionless time λ, we further obtain

$$\tilde{a}'(\lambda) = -\tfrac{4}{3}C\tilde{a}^{3/2}[\cos\varepsilon\sin\lambda\cos(\tilde{\omega}+\theta) - \cos\lambda\sin(\tilde{\omega}+\theta)], \tag{41}$$

The equation for $\tilde{a}$ is an equation with multiplicative noise and in terms of Stratonovich calculus, separation of variables yields the result

$$\begin{aligned}\tilde{a}_\mathrm{t}^{-1/2}(\lambda) - 1 = \frac{2}{3}\int_0^\lambda & [\cos\varepsilon\sin x\cos f(x) \\ & - \cos x\sin f(x)]C_\xi(x)\,\mathrm{d}x.\end{aligned} \tag{42}$$

The integrand contains the oscillatory function $f(x) = \tilde{\omega}(x) + \theta(x)$ which is a fast variable and hence, for $\lambda \gg 1$ may be accurately approximated by a uniform distribution. Since $C_\xi(x)$ is Gaussian, the resulting integral in the last equation is also Gaussian with zero mean and with variance equal to $4\Lambda\lambda/9$. Thus, we obtain

$$\begin{aligned}&\langle\tilde{a}_\mathrm{t}^{-1}(\lambda)\rangle = 1 + 4\Lambda\lambda/9, \\ &\langle\tilde{a}_\mathrm{t}^{-2}(\lambda)\rangle = 1 + 8\Lambda\lambda/3 + 16\Lambda^2\lambda^2/27\end{aligned} \tag{43}$$

or

$$\langle\tilde{a}_\mathrm{t}^{-2}(\lambda)\rangle - \langle\tilde{a}_\mathrm{t}^{-1}(\lambda)\rangle^2 = \tfrac{2}{9}\Lambda\lambda + \tfrac{32}{81}\Lambda^2\lambda^2. \tag{44}$$

Hence in a linear approximation the coefficient Λ in Eq. (44) plays a role of the diffusion constant for the dimensionless time λ. To compare the obtained result with the conclusion of the simplified analysis of Section 3, we notice that $\tilde{a}_\mathrm{t} = 1 + \delta a/a_0$ and that

$$\langle\tilde{a}_\mathrm{t}^{-2}(\lambda)\rangle - \langle\tilde{a}_\mathrm{t}^{-1}(\lambda)\rangle^2 = 2\frac{\langle(\delta a)^2\rangle}{a_0^2} = 2\Lambda\lambda/9, \tag{45}$$

where all non-linear terms have been omitted. Applying the definitions of λ and Λ, Eqs. (28) and (35), it is easy to show that the diffusion coefficient D of the simplified analysis, Eq. (26), coincides (up to a numerical prefactor) with the dimensionless coefficient Λ, if the dimensionless time is used.

4.4. General solution for inclination

It is known that the inclination components p and q in case of $\omega \ll 1$ (which corresponds to the case of Deimos ejecta for the circum-Martian motion), and $\omega \approx 1$ (which corresponds to the Phobos ejecta) have a different behaviour (Krivov et al., 1996). For simplicity in what follows we assume that $\omega \ll 1$.

In order to analyse the evolution of the inclination in the general case it is not enough to use orbit-averaged equations since they lack zeroth-order terms, which cause a noticeable diffusion. Following Burns (1976), we write the perturbation equation as

$$\mathrm{d}\vec{L}/\mathrm{d}t = \vec{r} \times F_{\mathrm{rp}}\vec{e}_{\odot}, \quad \vec{L} = \vec{r} \times m\vec{v}, \quad p = -L_y/L, \quad q = L_x/L, \tag{46}$$

with the angular momentum $\vec{L}$, where $L^2 = m^2 GMa(1-e^2)$.

Using an approximation $a \approx a_0$, we obtain after long but straightforward calculations

$$p'_{\mathrm{t}}(\lambda) = \tfrac{2}{3}C \sin\varepsilon \sin\lambda \sin(g+\theta) + \mathrm{O}_{1,p}(h,k,p,q), \tag{47}$$

$$q'_{\mathrm{t}}(\lambda) = \tfrac{2}{3}C \sin\varepsilon \sin\lambda \cos(g+\theta) + \mathrm{O}_{1,q}(h,k,p,q). \tag{48}$$

For the constant $C = C_{\mathrm{d}}$ the above zero-order terms can be neglected since their average over the orbit vanishes. These, however, give rise to a substantial diffusion when $C = C_{\mathrm{d}} + C_{\xi}(\lambda)$. It is possible to improve Eqs. (47) and (48) by adding first-order terms $\mathrm{O}_{1,p/q}$ from, for instance, orbit-averaged equations by Krivov et al. (1996), while still keeping the equations linear and thus analytically solvable. However, solutions of such more general equations are extremely cumbersome and do not add any important secular term to the moments of p_{t} and q_{t} (though the more general equations are needed for an accurate analytical estimate of p_{d} and q_{d} as demonstrated by Krivov et al., 1996).

Calculation of the moments of the inclination components from Eqs. (47) and (48) can be done in a very similar manner as presented for the eccentricity case (Appendix B). The inclination elements p_{t} and q_{t} are normally distributed, while $\sin i_{\mathrm{t}} = (p_{\mathrm{t}}^2 + q_{\mathrm{t}}^2)^{1/2}$ is not Gaussian. Their average read

$$\langle p_{\mathrm{t}}(\lambda)\rangle \approx p_{\mathrm{d}}(\lambda), \quad \langle q_{\mathrm{t}}(\lambda)\rangle \approx q_{\mathrm{d}}(\lambda), \tag{49}$$

and the standard deviations are

$$\langle p_{\mathrm{t}}^2(\lambda)\rangle - \langle p_{\mathrm{t}}(\lambda)\rangle^2 \approx \langle q_{\mathrm{t}}^2(\lambda)\rangle - \langle q_{\mathrm{t}}(\lambda)\rangle^2 \approx \Upsilon\Lambda, \tag{50}$$

where

$$\Upsilon \equiv \frac{8\sin^2\varepsilon}{9(3+\cos 2\varepsilon)}\Lambda. \tag{51}$$

Similarly

$$\langle \sin i_{\mathrm{t}}(\lambda)\rangle \approx \sqrt{\sin^2 i_{\mathrm{d}}(\lambda) + \alpha_i \Upsilon\Lambda}, \tag{52}$$

$$\langle \sin^2 i_{\mathrm{t}}(\lambda)\rangle - \langle \sin i_{\mathrm{t}}(\lambda)\rangle^2 \approx (2-\alpha_i)\Upsilon\Lambda, \tag{53}$$

$$\alpha_i = \begin{cases} 1/2, & \Upsilon\Lambda \ll \sin^2 i_{\mathrm{d}}, \\ \pi/2, & \Upsilon\Lambda \gg \sin^2 i_{\mathrm{d}}. \end{cases} \tag{54}$$

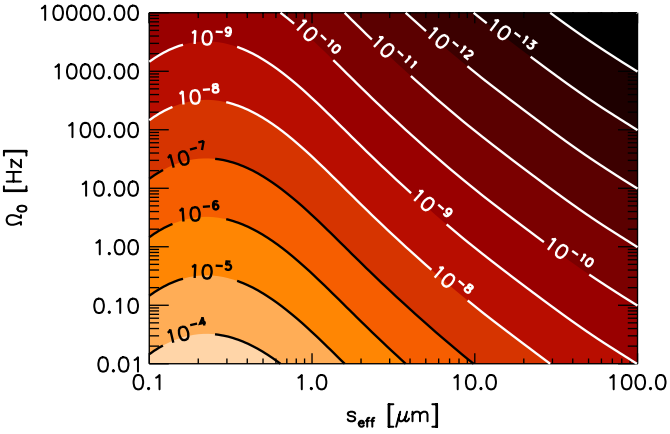

Fig. 2. Dependence of dimensionless diffusion coefficient Λ defined by Eq. (35) on the particle effective radius s_{eff} and the rotation velocity Ω_0. The calculations are done for an oblate silicate grain placed on the Deimos orbit. The bulk density of the grain is $\varrho_g = 2.37 \times 10^3\,\mathrm{kg/m^3}$, the aspect ratio is $\alpha = 5$ and the radiation pressure efficiency coefficient Q_{pr} was calculated for each grain size as described by Makuch et al. (2005). The non-monotonous behaviour of Λ stems from that of the coefficient Q_{pr}.

Here, we again encounter the diffusional behaviour of the orbital elements.

4.5. Diffusive behaviour of the orbital elements

As we have demonstrated above, all the orbital elements show a diffusive behaviour with the effective diffusive coefficients. These coefficients are proportional with the coefficient of the order of unity to the "basic" dimensionless coefficient Λ (see Eqs. (35), (37), (44), (50), (53)). The coefficient Λ sensitively depends on the particle's size s_{eff} and the rotational frequency Ω_0, as is illustrated in Fig. 2, where $\alpha = 5$ and the other parameters were taken for the circum-Martian motion on the Deimos orbit. In particular, we use $\varepsilon = 25^\circ$, $\omega = 0.0335$ (for details see Krivov et al., 1996), $\rho_g = 2.37\,\mathrm{g\,cm^{-3}}$ and Q_{pr} was calculated according to the grain effective radius as discussed by Makuch et al. (2005). As it follows from Fig. 2, the coefficient Λ varies by 10 orders of magnitude in the range of astrophysically relevant values for s_{eff} and Ω_0. The non-monotonous behaviour of Λ stems from that of the radiation pressure efficiency coefficient Q_{pr} (Makuch et al., 2005).

As it will be shown below, the analytical theory for the diffusion coefficients gives the lower boundary for this value, hence Fig. 2 may be used to estimate the impact of the stochastic radiation pressure. Note that the results of the plot may also be used for a rough estimate of the low boundary of the effect for a general circumplanetary motion, after the proper rescaling of the distance of the planet from the Sun a_{plan} (scales as a_{plan}^{-4}), the mass of the planet M (scales as M^{-1}) and the semimajor axis (scales as a_0).

5. Numerical simulations: application for the circum-Martian dynamics

To check the predictions of the analytical theory we perform a set of numerical simulations for the particular case of circumplanetary dynamics. Namely, in what follows we focus on the circum-Martian motion of dust ejected from Deimos. Choosing the grain size we take into account its astrophysical relevance. Namely, according to the classification by Krivov (1994) there exist several groups of particles with quite different dynamics. The biggest ejecta fragments, larger than approximately 1 mm (denoted as Population 0), are only subject to the gravity of the oblate planet. They create narrow tori along the moons' orbits. Since these particles are rapidly lost due to collisions with the parent moons, their lifetimes and corresponding number densities are very small. Smaller grains, which sizes range from tens to hundreds of micrometers form Population I and are small enough to be noticeably affected by non-gravitational perturbing forces, such as direct radiation pressure and Poynting–Robertson effect. The lifetimes of these grains are between tens of years (Phobos' ejecta) and tens of thousands years (Deimos). They form extended asymmetric tori and are expected to be the main component of the Martian dust environment. The most important loss mechanism of these dust particles is the re-accretion by the parent moon as well as the mutual collisions as shown in the recent study by Makuch et al. (2005). The combined influence of planetary oblateness and radiation pressure causes periodic oscillations of eccentricity and inclination. Since the maximal eccentricity is inversely proportional to the particle size (Krivov et al., 1996), there exist a critical grain size $s_{\rm crit}$ ($\approx 10\,\mu$m) below which the particles hit Mars at the pericentre of their orbit in less than one year. These micron-sized grains form Population II. Still smaller, submicron-sized particles (Population III) are strongly affected by fast fluctuations of the solar wind and plasma environment. They are swept out from the vicinity of Mars within 10–100 days and form a highly variable subtle halo around Mars (Horányi et al., 1990, 1991).

Based on rather robust theoretical predictions there were a couple of attempts to detect the Martian dust tori (see Krivov et al., 2006 for a review). However, none of them have been successful up to now. We are motivated by these negative results to reconsider the dynamics of dust particles and to find a mechanism changing the predicted optical properties of the tori. Therefore, in the present study we apply our general theory to describe the dynamics of Population I, which is expected to be the most dominant in the Martian system (Juhász and Horányi, 1995). The long lifetimes of these particles implies that even weak perturbations may cause a significant change of the tori characteristics. The dynamics of the tori particles under the influence of planetary oblateness (J2), direct radiation pressure (RP), and Poynting–Robertson drag (PR) was studied in detail (Krivov et al., 1996; Hamilton, 1996; Ishimoto, 1996; Krivov and Hamilton, 1997; Makuch et al., 2005). However, any impact of stochastic perturbations has never been addressed before in the context of this problem.

To model the stochastic dynamics of these particles we consider an ensemble of oblate grains with the bulk density of $2.37\times10^3\,\mathrm{kg/m^3}$ corresponding to silicate. Assuming ergodicity, the dynamics of a single grain mimics the evolution of the whole ensemble. We have tested a wide range of parameters $s_{\rm min}$, α, and Ω_0, which characterize the properties of the grains. As has been already mentioned, the radiation pressure efficiency coefficient $Q_{\rm pr}$ was calculated according to the approach presented by Makuch et al. (2005). The initial elements were identical for all ejected particles. The starting position was a circular orbit lying in the equatorial plane with a semimajor axis a equal to that of Deimos (23 480 km).

To trace the dynamics of the ejected grains we numerically integrated Eq. (1) of planetocentric particles subject to gravity of oblate Mars and stochastic radiation pressure force (2). We used the constant integration time step $\Delta t = 500$ s. At each integration step the calculated coordinates and velocities were converted into the osculating orbital elements and stored. As described previously, the radiation pressure force consists of two components. The first, deterministic part is the direct radiation pressure. It acts on a particle with the average cross-section defined by Eq. (13). The second, stochastic part was modelled by a Gaussian white noise. The method of modelling of the stochastic component is similar to that used by Spahn et al. (2003). At each integration step a random Gaussian variable with zero mean and unit variance was generated. Than it was scaled by a numerical factor κ and added to the deterministic part of the radiation pressure. This numerical scheme, so-called "exact propagator", is described in detail in Mannella (2000) and in Mannella and Palleschi (1989). With the factor κ defined as

$$\kappa = B\frac{1}{\Delta t}\sqrt{2K_0\Delta t} \tag{55}$$

this numerical scheme yields the accuracy of the order of the integration time step Δt. We want to stress here that the factor κ in Eq. (55) reflects the amplitude of the noise, which is inversely proportional to the square root of the rotation frequency (see definition of K_0, Eq. (14)). Note also that the preceding factor $1/\Delta t$ in the right-hand side of Eq. (55) comes into play since we add the stochastic radiation pressure into the integration routine for the deterministic part (see Mannella, 2000, for the detail). We additionally checked our numerical results on shorter timescales (up to hundreds of M.y.) using another stochastic integrator (Milstein et al., 2002).

Here we present the results of numerical simulations for two different particle sizes with the effective radius $s_{\rm eff}$ of 15 and 40 μm. As it has been already noted the minimal particle radius can be calculated for oblate particles from the relation, $l = s_{\rm min} = s_{\rm eff}\sqrt{2/\alpha(\alpha+1)}$. Since our main

goal is to compare the simulation results with the predictions of the analytical theory, we chose a relatively short integration time of less than 3000 Martian years. The results of longer simulations with larger variety of particle sizes, shape, and spin properties will be presented elsewhere. In each run we performed a series of realizations of the stochastic radiation pressure, i.e. a set of individual orbits with identical initial orbits has been simulated. In our simulations we studied the oblate particles with the aspect ratio $\alpha = 5$. The radiation pressure coefficient of $Q_{\rm pr} = 0.385$ ($s_{\rm eff} = 15\,\mu$m) and $Q_{\rm pr} = 0.372$ ($s_{\rm eff} = 40\,\mu$m) was used (see Table 1).

We expect that for the case of circum-Martian motion the angular velocity of the grains is determined by the ejection mechanism, for which our simple model yields $\Omega_0 = 5 \times 10^3\,{\rm s}^{-1}$ (see Section 3.2). Therefore in simulations we mainly use this value of Ω_0. However, some unaccounted processes during the dust creation may not be excluded, which imply the other magnitude of Ω_0. Hence for the case of $s_{\rm eff} = 15\,\mu$m we also use $\Omega_0 = 1.5 \times 10^{-2}\,{\rm s}^{-1}$ as an alternative value of the rotation frequency.

As it follows from our studies, the permanent action of the stochastic perturbation causes a spatial spread of particle trajectories. The spread itself can be characterized by a standard deviation of the osculating elements. The time dependence of the standard deviation of the orbital elements of the ensemble of 200 and more particles with the effective radii $s_{\rm eff} = 40$ and $15\,\mu$m are shown in Figs. 3–5. The predictions of the analytical theory are also plotted along with the numerical results. The corresponding

Table 1
Numerical values of the constants characterizing the diffusion of orbital elements derived from the analytical predictions, for a given particle size and aspect ratio $\alpha = 5$

$s_{\rm eff}$ (μm)	$Q_{\rm pr}$	Ω_0 (Hz)	σ^2	$C_{\rm d}$	Λ	Υ
40	0.372	5×10^3	2.3×10^{-14}	0.061	1.0×10^{-14}	4.5×10^{-16}
15	0.385	5×10^3	1.8×10^{-13}	0.166	8.0×10^{-14}	3.5×10^{-15}
15	0.385	1.5×10^{-2}	5.8×10^{-8}	0.166	2.7×10^{-8}	1.2×10^{-9}

Direct comparison with the numerical simulations is depicted in Figs. 3–5.

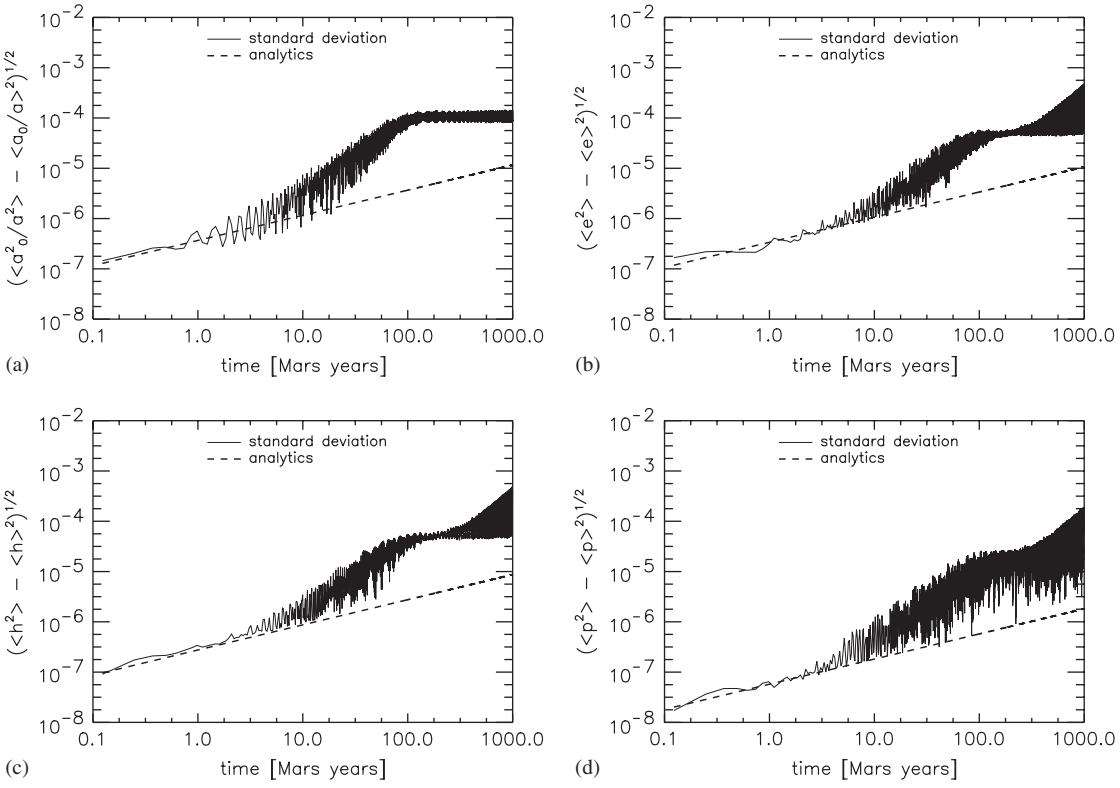

Fig. 3. The standard deviations of: (a) normalized inverse semimajor axis; (b) eccentricity; (c) Lagrangian element $h = e\cos\tilde{\omega}$; and (d) Lagrangian element $p = \sin i \cos\Omega$ for an ensemble of 200 particles. The time dependence of the orbital elements k and q is almost identical to that of h and p, respectively, and hence is not shown. Parameters of the grains are: $s_{\rm eff} = 40\,\mu$m, the aspect ratio $\alpha = 5$, and the rotation frequency $\Omega_0 = 5 \times 10^3\,{\rm s}^{-1}$. The dashed line depicts the analytical estimates.

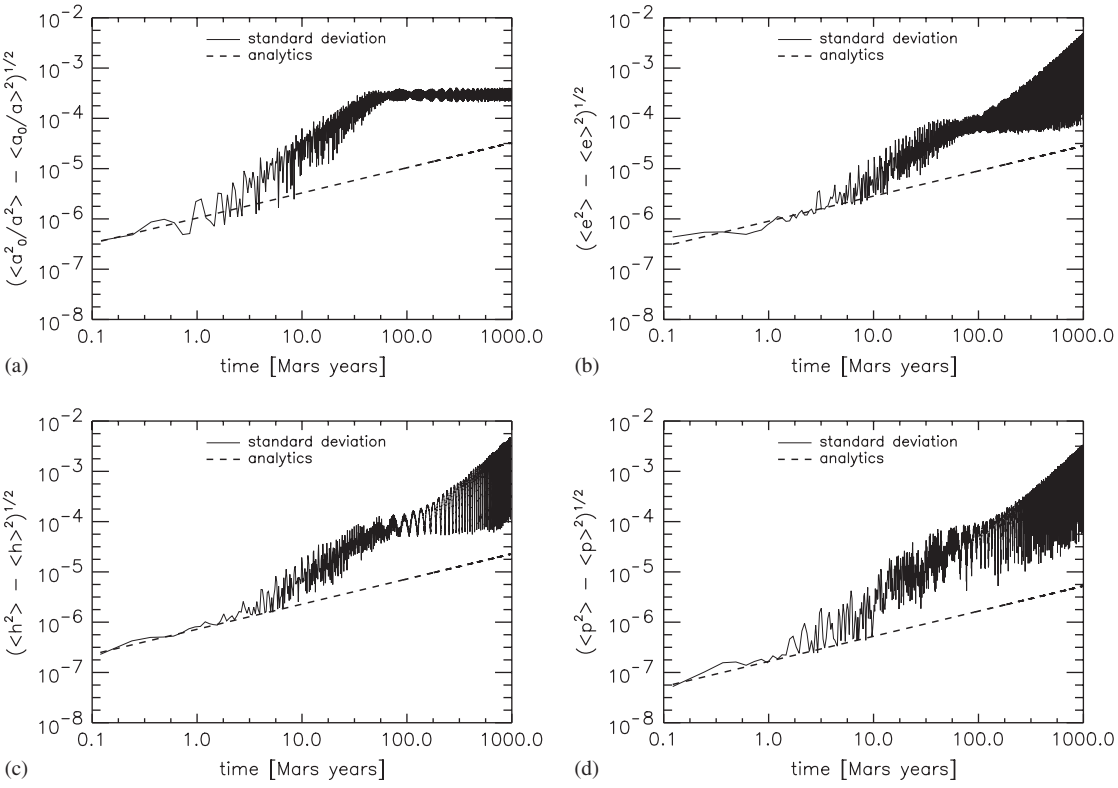

Fig. 4. The same as Fig. 3, but for particle size $s_{\mathrm{eff}} = 15\,\mu\mathrm{m}$.

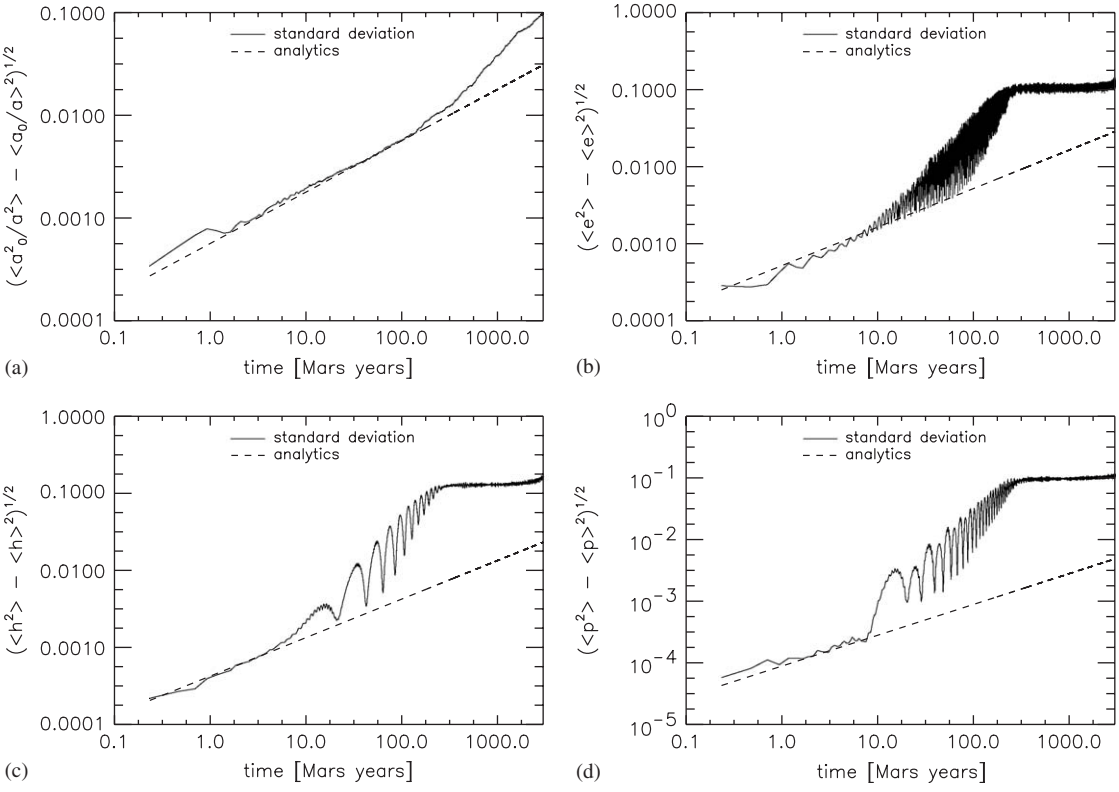

Fig. 5. The same as Fig. 3, but for particle size $s_{\mathrm{eff}} = 15\,\mu\mathrm{m}$ and $\Omega_0 = 1.5 \times 10^{-2}$.

analytical values of σ^2, diffusion coefficients Λ, Υ, and the deterministic component of radiation pressure C_d for a used grain size and Ω_0 are given in Table 1.

Comparing the numerical results for the both grain sizes, Figs. 3 and 4, it is evident that the dispersion of the elements depends on the particle size: the grains with smaller size are more sensitive to the influence of a stochastic radiation pressure and the corresponding dispersion of trajectories is higher. Moreover, from Figs. 4 and 5 it may also be seen that the spatial spread of the trajectories crucially depends on the rotational frequency Ω_0. While for the large Ω_0 the spread is relatively weak (Figs. 3 and 4), for the case of slow rotation (Fig. 5) a significant variation of the orbital elements, up to 10% during the first 1000 years, is observed.

The agreement between the analytical predictions and simulation results is good at the beginning of the ensemble evolution. Later, however, a noticeable deviation of the theory from the numerical results is observed. This may be attributed to the neglected non-linear terms, becoming important in course of time. At this point we face the limitation of our theory due to initial assumptions taken in order to proceed such complex problem. These are e.g. the condition of mutual independence of the elements or limitations of the linear theory. Comparing the plots for different grain sizes one can notice that the accuracy of the theory crucially depends on the deterministic coefficient C_d, which is inversely proportional to the size of the grains.

We wish to stress that although our analytical theory fails at later times, it presumably gives the low boundary estimate for the effect of interest. In other words, due to the omitted non-linear terms, the actual standard deviation of the orbital elements is always larger than that predicted by the analytical theory. The other interesting effects which may be attributed to the omitted non-linear terms are the apparent saturation of the standard deviation of the orbital elements (Figs. 3a and 4a) and alternation of their regime of growth (Figs. 3b and 4b). The latter effect lacks presently an explanation, while the former one may be interprete as follows: the detailed analysis (Brilliantov et al., 2006) shows that the form of simplified Gauss perturbation equations after their linearization is similar to that of the *damped* stochastic oscillator. The standard deviation of the amplitude of the latter system saturates after an initial linear growth with time. In our analytical approach which, is aimed to obtain the estimates of the effective diffusion coefficients, we omit for simplicity very small terms, responsible for the damping. Hence our theory corresponds to the *undamped* stochastic oscillator which lacks the saturation, whereas the numerical study successfully reproduces the saturation effect.

6. Conclusions

We analyse the role of stochastic perturbations in the circumplanetary motion of dust particles. We address one of the most important sources of the stochasticity in this system—the random modulation of the radiation pressure force by the rotation motion of non-spherical particles. We formulate the model of the stochastic radiation pressure based on this effect. We consider particles of a simplified form, that is, we assume the particles to be the figures of rotation. These may be characterized by two dimensions, one parallel to the symmetry axis and the other one, perpendicular to this axis. Such simplified model allows to express the stochastic properties of the fluctuating radiation pressure in terms of the rotational time-correlation function of rotating grains. In order to calculate the time-correlation function we adopt a model of freely rotating particles, whose dependence on time is determined by a characteristic angular velocity. According to our estimates, the particles perform a very fast rotation around their centre of mass on the timescale of the orbital motion. This allows to represent the radiation pressure force as a sum of a deterministic component, which refers to the average cross-section of the spinning particles and a random component, modelled as a Gaussian white noise with zero mean. The dispersion of the noise is expressed in terms of the time integral of the orientational time-correlation function. We estimate the characteristic rotation frequency for two different mechanisms of particle creation, one due to the impact-ejection mechanism by hypervelocity impacts of interplanetary particles and the other one due to volcanic eruption of a dust–gas mixture.

We performed numerical and analytical studies of the formulated model of the stochastic radiation pressure. In the analytical treatment we expanded the equations of motion around the initial orbit and kept terms up to the second order in this expansion. To treat the stochastic terms in the simplified equations we applied Stratonovich calculus and obtain the solution to these stochastic differential equations. Using the properties of the Gaussian white noise we derived expressions for the average and square average of the orbital elements for the ensemble of non-spherical particles. Our results clearly demonstrate the diffusion-like behaviour of these quantities. We also find explicit expressions for the effective diffusion coefficients which characterize the growth rate of the standard deviations of the orbital elements.

The analytical results have been compared with results of extensive numerical simulations with the parameters corresponding to the motion on the Deimos orbit around Mars. We observe that the predictions of our theory are in a very good agreement with the simulation results for the initial period of the system evolution. The agreement however worsens at later times due to the increasing impact of the non-linear terms neglected in the theoretical approach. We conclude that our analytical theory may be used for an estimate of the low boundary of the time-dependent standard deviation of the orbital elements. Since the simulation of orbital motion with stochastic forces is extremely time consuming, all numerical runs have been performed only for a restricted interval of time, less than 3000 Martian years. Nevertheless, even for this, relatively

short time, the effect of the stochastic radiation pressure has been found to be significant.

Therefore, the results of our study lead us to the conclusion that the stochasticity of the radiation pressure force due to the rotation of non-spherical particles plays a significant role in the orbital dynamics of dust grains and may be crucial in determining the density distribution of dusty systems, especially the Martian dust tori.

Acknowledgements

We thank Nicole Albers for her careful corrections of this manuscript and together with Jürgen Schmidt for useful comments and stimulating discussions. This research was funded by Deutsche Forschungsgemeinschaft (DFG), projects Kr 2164/1-3 (M.M.) and Sp 384/18-1 (N.V.B.). M.S. was supported by Cassini UVIS project.

Appendix A. Time-correlation function of rotation motion

In this section the details of the evaluation of the time-correlation function $K(t)$ are discussed for the case of *prolate* particles. Using Eq. (9) we write the average cross-section as

$$\langle S_r\rangle = 4Ll\langle\sin\theta(t)\rangle + \pi l^2 = \pi l(L+l) \tag{A.1}$$

and, respectively, fluctuation as

$$\xi(t) = S(t) - \langle S\rangle = 4Ll\left(\sin\theta(t) - \frac{\pi}{4}\right), \tag{A.2}$$

where we take into account that the angle θ is uniformly distributed over the sphere with the density $1/4\pi$:

$$\langle\sin\theta(t)\rangle = \int_0^{\pi}\sin\theta\,\mathrm{d}\theta\int_0^{2\pi}\mathrm{d}\varphi\,\frac{1}{4\pi}\sin\theta = \frac{\pi}{4}. \tag{A.3}$$

Similarly, for the uniform distribution $\langle\sin^2\theta(t)\rangle = \frac{2}{3}$. Hence, the time-correlation function $K(t)$ may be written as

$$\langle\xi(0)\xi(t)\rangle = L^2l^2(\tfrac{32}{3} - \pi^2)k(t) = K(0)k(t), \tag{A.4}$$

with the normalized time-correlation function

$$k(t) = \frac{\langle\sin\theta(0)\sin\theta(t)\rangle - \langle\sin\theta\rangle^2}{(32/3-\pi^2)}, \tag{A.5}$$

so that $k(0) = 1$. We wish to note that the free-rotators model for the orientational motion is used to obtain *qualitative* estimates. This simplest model is not, however, a self-averaging model: although $\langle\xi\rangle = 0$, the asymptotic value of the time-correlation function for this model at $t\to\infty$ does not vanish, $\langle\xi(0)\xi(\infty)\rangle \neq 0$ (see e.g. Binder and Heermann, 1983, for more precise definition). This property of the ensemble of free rotators has been already pointed out by Pierre and Steele (1969). Still, one can exploit this model, either subtracting from $k(t)$ its asymptotic value, $k(t)\to k(t) - k(\infty)$, or using the *model function*, according to the rule, suggested by Pierre and Steele (1969):

$$k(t) \approx \mathrm{e}^{-\varkappa t^2/2}, \quad \varkappa = -\frac{\mathrm{d}^2}{\mathrm{d}t^2}k(t)\bigg|_{t=0}. \tag{A.6}$$

This Gaussian model function satisfies the basic requirements for the time-correlation functions, $\mathrm{d}k(t)/\mathrm{d}t = 0$ at $t = 0$ and $k(\infty) = 0$ (see e.g. Brilliantov and Revokatov, 1996). It has been also shown by Pierre and Steele (1969) that it mimics rather satisfactory the actual correlation function $k(t)$.

To find $k(t)$ one needs to know how $\sin\theta(t)$ depends on time for an individual particle and then perform the ensemble averaging. Since there is no external torque exerted on the particles, this is completely kinematical problem. According to the elementary mechanics (e.g. Landau and Lifshitz, 1965) the motion of such particles corresponds to the motion of a free symmetric top. That is, the angular momentum of the particle $\vec{M}$ is kept fixed, while the body performs two superimposed rotations: it rotates around its symmetry axis and the symmetry axis itself precesses around the vector $\vec{M}$, with the angular velocity Ω_{pr} (see Fig. 6). The rotation around the symmetry axis does not change the angle θ and hence can be neglected; θ is, however, affected by the precession.

Let the components of the inertia tensor in its principal axes, x', y', z', be $I_1 = I_2 = I_\perp$ and $I_3 = I_\parallel$ (the symmetry axis is directed along z'-axis), and the components of the angular velocity be Ω_1, Ω_2, and Ω_3, then the angular momentum reads as

$$M = \sqrt{(I_\perp\Omega_1)^2 + (I_\perp\Omega_2)^2 + (I_\parallel\Omega_3)^2}. \tag{A.7}$$

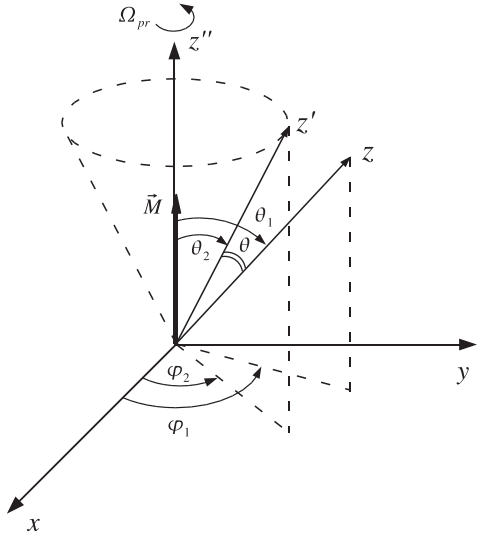

Fig. 6. Shows the relative orientation of the angular momentum of a particle $\vec{M}$, the symmetry axis of the particle z' and the "fixed-frame" z-axis, directed along the vector $\vec{e}_\odot$. In the coordinate system with M directed along z''-axis, the azimuthal and polar angles for the directions z and z' are, respectively, θ_1, φ_1 and θ_2, φ_2.

Correspondingly, the precession angular velocity may be written as (see e.g. Landau and Lifshitz, 1965)

$$\Omega_{\rm pr} = \frac{M}{I_\perp} = \sqrt{\Omega_1^2 + \Omega_2^2 + \beta^2\Omega_3^2}, \tag{A.8}$$

where $\beta \equiv I_\parallel / I_\perp$.

For (prolate) particles of a uniform density ϱ_g the principal components of the inertia tensor read as

$$I_\parallel = \pi\varrho_g l^5(\alpha + \tfrac{8}{15}),$$
$$I_\perp = \tfrac{1}{2}\pi\varrho_g l^5[\alpha(1 + \tfrac{4}{3}\alpha^2) + \tfrac{8}{15}(\alpha + \tfrac{3}{8})^2]. \tag{A.9}$$

Hence, the coefficient β, which defines the precession frequency, depends on the aspect ratio α as

$$\beta = \frac{2\alpha + 16/15}{\alpha(1 + 4\alpha^2/3) + (8/15)(\alpha + 3/8)^2}. \tag{A.10}$$

Let the angle between z-axis of the fixed frame, which is directed along the vector $\vec{e}_\odot$ and the angular momentum $\vec{M}$ be θ_1, while the angle between $\vec{M}$ and the symmetry axis z' of the particle be θ_2. Since the symmetry axis z' makes a precession with a constant angular velocity $\Omega_{\rm pr}$ around $\vec{M}$, the angle $\varphi(t)$ between the projection of the z-axis on the plane perpendicular to the vector $\vec{M}$ and projection of the symmetry axis z' on the same plane (see Fig. 6) evolves in time as

$$\varphi(t) = \varphi_1 - \varphi_2 = \varphi_0 + \Omega_{\rm pr} t, \tag{A.11}$$

where φ_0 is some initial angle (see Fig. 6). According to the elementary geometry, the angle θ between the z-axis and the symmetry axis z' may be expressed in terms of the above angles as

$$\cos\theta(t) = \cos\theta_1\cos\theta_2 + \sin\theta_1\sin\theta_2\cos\varphi(t), \tag{A.12}$$

where the angles θ_1 and θ_2 do not change with time for a freely rotating particle. Correspondingly, we can write, $\sin\theta(t) = \sqrt{1 - \cos^2\theta(t)}$.

Due to the symmetry of the problem it is reasonable to assume that the direction of the vector $\vec{M}$ with respect to z-axis as well as the direction of the symmetry axis with respect to the $\vec{M}$ are spherically symmetric, that is we assume the following distribution functions:

$$P(\theta_1, \varphi_1) = P(\theta_2, \varphi_2) = \frac{1}{4\pi}. \tag{A.13}$$

Finally, we need the angular velocity distribution function, which characterizes the ensemble of rotating particles. It is natural to assume that the rotation energy of particles is distributed according to a Gaussian distribution, with a characteristic angular velocity Ω_0 and that the equipartition between the rotational degrees of freedom holds: $\langle I_1\Omega_1^2/2\rangle = \langle I_2\Omega_2^2/2\rangle = \langle I_3\Omega_3^2/2\rangle = I_\perp\Omega_0^2/2$. Then the normalized distribution function reads as

$$f(\Omega_1, \Omega_2, \Omega_3) = \frac{\sqrt{\beta}}{\Omega_0^3\pi^{3/2}} \exp\left[-\frac{\Omega_1^2 + \Omega_2^2 + \beta\Omega_3^2}{\Omega_0^2}\right]. \tag{A.14}$$

As the result we obtain for the time-correlation function $\langle\sin\theta(t)\sin\theta(0)\rangle$:

$$\begin{aligned}\langle\sin\theta(t)\sin\theta(0)\rangle &= \left(\frac{1}{4\pi}\right)^2 \int_0^\pi \sin\theta_1\,{\rm d}\theta_1 \int_0^{2\pi} {\rm d}\varphi_1 \int_0^\pi \sin\theta_2\,{\rm d}\theta_2 \int_0^{2\pi} {\rm d}\varphi_2 \\ &\times \frac{\sqrt{\beta}}{\Omega_0^3\pi^{3/2}} \int_{-\infty}^\infty {\rm d}\Omega_1 \int_{-\infty}^\infty {\rm d}\Omega_2 \int_{-\infty}^\infty {\rm d}\Omega_3 \\ &\times \exp\left[-\frac{\Omega_1^2 + \Omega_2^2 + \beta\Omega_3^2}{\Omega_0^2}\right] \\ &\times \sqrt{1 - \cos^2[\theta(0)]}\sqrt{1 - \cos^2[\theta(t)]},\end{aligned} \tag{A.15}$$

where $\cos\theta(t)$ is given by Eq. (A.12) with $\varphi(t)$ expressed in terms of the precession angular velocity by Eq. (A.11).

Noticing that the integration over Ω_i, $i = 1, 2, 3$ in the last equation may be performed in terms of dimensionless variables $\omega_i = \Omega_i/\Omega_0$, and that the precession angular velocity may be written as $\Omega_{\rm pr} = \Omega_0(\omega_1^2 + \omega_2^2 + \beta^2\omega_3^2)^{1/2}$. One concludes that the correlation function $\langle\sin\theta(t)\sin\theta(0)\rangle$ and hence the function $k(t)$, indeed, depends on time through the product $\Omega_0 t$ (see Eqs. (A.11), (A.12)). Similar conclusion about the orientational correlation function for an ensemble of freely rotating symmetric tops has been made by Pierre and Steele (1969) and by Guissani et al. (1977). In these papers somewhat different orientational correlation functions were studied. These also depended on the product $\Omega_T t$, where Ω_T is the characteristic angular velocity of molecular gas, which is also called thermal velocity. Unfortunately, it is not possible to obtain an analytical expression for these correlation functions, even for the simpler case addressed in the over-mentioned papers.

However, one can use the model correlation function $k(t)$, defined in Eq. (A.6). The calculation detail will be published elsewhere, here we present only the final result,

$$\begin{aligned}\varkappa &= -\frac{{\rm d}^2}{{\rm d}t^2}k(t)\bigg|_{t=0} = -(32/3 - \pi^2)^{-1}\frac{{\rm d}^2}{{\rm d}t^2}\langle\sin\theta(t)\sin\theta(0)\rangle\bigg|_{t=0} \\ &= 0.138(1 + \beta/2)\Omega_0^2,\end{aligned} \tag{A.16}$$

where the aspect-ratio-dependent parameter β is given by Eq. (A.10). Finally, we obtain the time integral of the correlation function $k(t)$ which is needed to find K_0 (see Section 3.2):

$$\begin{aligned}A\Omega_0^{-1} &= \int_0^\infty k(t)\,{\rm d}t = \int_0^\infty {\rm e}^{-\varkappa t^2/2}\,{\rm d}t = \sqrt{\frac{\pi}{2\varkappa}} \\ &= \left(\frac{3.37}{\sqrt{1 + \beta/2}}\right)\Omega_0^{-1}.\end{aligned} \tag{A.17}$$

Calculations of this quantity for the case of oblate particles are more involved, therefore we use presently the approximation $A \approx 1$ for these particles.

Appendix B. Integration of the stochastic orbit-averaged equations

B.1. Orbit-averaged equations of motion

The orbit-averaged equations of motion of particles governed by J2 (oblateness) and RP (radiation pressure) read (Krivov et al., 1996)

$$\frac{\mathrm{d}h}{\mathrm{d}\lambda} = -k\omega\frac{5I^2-2I-1}{2E^4} - \frac{C}{E(1+I)}\{[p-Hh]q\cos\lambda + [E^2(1+I)-p(p-Hh)]\cos\varepsilon\sin\lambda + [E^2(1+I)p-IKk]\sin\varepsilon\sin\lambda\}, \tag{B.1}$$

$$\frac{\mathrm{d}k}{\mathrm{d}\lambda} = h\omega\frac{5I^2-2I-1}{2E^4} + \frac{C}{E(1+I)}\{[q-Hk]p\cos\varepsilon\sin\lambda + [E^2(1+I)-q(q-Hk)]\cos\lambda - [E^2(1+I)q-IKh]\sin\varepsilon\sin\lambda\}, \tag{B.2}$$

$$\frac{\mathrm{d}p}{\mathrm{d}\lambda} = q\omega\frac{I}{E^4} + \frac{C}{E(1+I)}[Hp-(1+I)h] \times[(p\cos\varepsilon - I\sin\varepsilon)\sin\lambda - q\cos\lambda], \tag{B.3}$$

$$\frac{\mathrm{d}q}{\mathrm{d}\lambda} = -p\omega\frac{I}{E^4} + \frac{C}{E(1+I)}[Hq-(1+I)k] \times[(p\cos\varepsilon - I\sin\varepsilon)\sin\lambda - q\cos\lambda], \tag{B.4}$$

with

$$E=\sqrt{1-e^2}=\sqrt{1-h^2-k^2},\quad I=\cos i=\sqrt{1-p^2-q^2},$$
$$H=hp+kq,\quad K=hq-kp, \tag{B.5}$$

where ε denotes the obliquity of a planet (e.g. 25° for Mars) and C and ω are dimensionless parameters that characterize the strength of radiation pressure and oblateness (see Krivov et al., 1996, for the exact definition). The other notation are the same as in Section 4.

B.2. Integration of the stochastic equations

Formally integrating Eqs. (32) for the purely random case, $C = C_\xi(\lambda)$ we obtain

$$h_\xi(\lambda) = \int_0^\lambda [\cos x\sin(\omega x-\omega\lambda) - \cos\varepsilon\sin x\cos(\omega x-\omega\lambda)]C_\xi(x)\,\mathrm{d}x, \tag{B.6}$$

$$k_\xi(\lambda) = \int_0^\lambda [\cos x\cos(\omega x-\omega\lambda) + \cos\varepsilon\sin x\sin(\omega x-\omega\lambda)]C_\xi(x)\,\mathrm{d}x, \tag{B.7}$$

where the Stratonovich calculus is assumed.[2] The latter relations read in a short notation

$$X_\xi(\lambda) = \int_0^\lambda F_X(\lambda,x)C_\xi(x)\,\mathrm{d}x, \tag{B.8}$$

where $X=\{h,k\}$. The integrands in Eqs. (B.6) and (B.7) are normally distributed random variables, hence the integrals are normally distributed as well. Since $\langle C_\xi\rangle = 0$, the mean values are zero, $\langle h_\xi\rangle = \langle k_\xi\rangle = 0$, while the second moments read as

$$\langle X_\xi(\lambda)Y_\xi(\lambda)\rangle = \sigma^2\int_0^\lambda F_X(\lambda,x)F_Y(\lambda,x)\,\mathrm{d}x,\quad X,Y=\{h,k\}. \tag{B.9}$$

The straightforward evaluation of the integral in the last equation yields rather lengthy result, which for $\lambda\gg 2\pi$ takes a simple form

$$\langle h_\xi^2(\lambda)\rangle \approx \langle k_\xi^2(\lambda)\rangle \approx \Lambda\lambda + \mathrm{O}(\sigma^2),$$
$$\langle h_\xi(\lambda)k_\xi(\lambda)\rangle \approx \mathrm{O}(\sigma^2), \tag{B.10}$$

where Λ is defined in Eq. (35) and the results have been obtained neglecting purely oscillatory terms.

The moments h_ξ^2 and k_ξ^2 are distributed according to the Gamma distribution with the parameter $\frac{1}{2}$ (also known as χ^2 distribution), or in compact notation $h_\xi^2 \sim \Gamma_{1/2}[2\Lambda\lambda]$. Although h_ξ and k_ξ are generally not independent, we may ignore their covariance as soon as $\lambda\gg 1$. Then $e_\xi^2 = h_\xi^2 + k_\xi^2$ is sum of two independent Γ-variates, which also gives a Γ-random number with the same scale factor, $2\Lambda\lambda$, while its parameter is sum of two initial parameters, or in short notation $e_\xi^2 \sim \Gamma_1[2\Lambda\lambda]$. Finally, for the eccentricity e_ξ we obtain that it is distributed in accordance with the Rayleigh distribution,

$$f(e_\xi) = \frac{e_\xi}{\Lambda\lambda}\exp\left[-\frac{e_\xi^2}{2\Lambda\lambda}\right],\quad \langle e_\xi(\lambda)\rangle = \sqrt{\pi\Lambda\lambda/2},$$
$$\langle e_\xi^2(\lambda)\rangle = 2\Lambda\lambda. \tag{B.11}$$

Due to the linearity of Eq. (32) the total solution reads $h_\mathrm{t} = h_\mathrm{d} + h_\xi$ and $k_\mathrm{t} = k_\mathrm{d} + k_\xi$, and Eqs. (33) and (34) are easy to verify. Similarly, the second moment of eccentricity is $\langle e_\mathrm{t}^2(\lambda)\rangle = e_\mathrm{d}^2(\lambda) + 2\Lambda\lambda$, but the calculation of the mean

$$\langle e_\mathrm{t}\rangle = \langle (h_\mathrm{t}^2+k_\mathrm{t}^2)^{1/2}\rangle = \langle [(h_\mathrm{d}+h_\xi)^2 + (k_\mathrm{d}+k_\xi)^2]^{1/2}\rangle \tag{B.12}$$

cannot be carried out explicitly since its components h_t and k_t have a non-zero mean. Instead, in the case of $\Lambda\lambda \gg e_\mathrm{d}^2$ using Taylor expansion we approximate the first moment by

$$\langle e_\mathrm{t}(\lambda)\rangle \approx (e_\mathrm{d}^2(\lambda) + \langle e_\xi\rangle^2)^{1/2} = (e_\mathrm{d}^2(\lambda) + \pi\Lambda\lambda/2)^{1/2}. \tag{B.13}$$

In the opposite case $\Lambda\lambda \ll e_\mathrm{d}^2$ a similar expression may be obtained with the numerical factor $\frac{1}{2}$ in place of $\pi/2$. Hence we arrive at Eq. (37).

[2] The choice of the Stratonovich calculus is appropriate here as the derivation of the perturbation equations uses the ordinary differentiation chain rule, as opposed to Ito calculus (see, for instance, Gardiner, 1983).

References

Binder, K., Heermann, D.W., 1983. Monte Carlo Simulations in Statistical Physics. Springer, Berlin.

Brilliantov, N.V., Revokatov, O.P., 1996. Molecular Motion in Disordered Media. Moscow University Press, Moscow (in Russian).

Brilliantov, N.V., Sremčević, M., Makuch, M., Spahn, F., 2006. Rotation dynamics of dust particles. Preprint.

Burns, J.A., 1976. Elementary derivation of the perturbation equations of celestial mechanics. Amer. J. Phys. 44, 944–949.

Burns, J.A., Lamy, P.L., Soter, S., 1979. Radiation forces on small particles in the Solar System. Icarus 40, 1–48.

Burns, J.A., Showalter, M.R., Morfill, G.E., 1984. In: Greenberg, R., Brahic, A. (Eds.), Planetary Rings. University of Arizona Press, Tucson, pp. 200–272.

Dikarev, V.V., 1999. Dynamics of particles in Saturn's E ring: effects of charge variations and the plasma drag force. Astron. Astrophys. 346, 1011–1019.

Esposito, L.W., Brahic, A., Burns, J.A., Marouf, E.A., 1991. Particle properties and processes in Uranus' rings. Uranus, 410–465.

Everhart, E., 1985. An efficient integrator that uses Gauss–Radau spacing. In: Carusi, A., Valsecchi, G.B. (Eds.), Dynamics of Comets: Their Origin and Evolution. Dordrecht, Reidel, pp. 185–202.

Gardiner, C.W., 1983. Handbook of Stochastic Methods. Springer, Berlin, Heidelberg.

Guissani, Y., Leicknam, J.C., Bratos, S., 1977. Vectorial correlation functions for a classical system of free asymmetric rotors. Phys. Rev. A 16 (5), 2072–2079.

Hamilton, D.P., 1996. The asymmetric time-variable rings of Mars. Icarus 119, 153–172.

Horányi, M., Burns, J.A., Tatrallyay, M., Luhmann, J.G., 1990. Toward understanding the fate of dust lost from the Martian satellites. Geophys. Res. Lett. 17, 853–856.

Horányi, M., Tátrallyay, M., Juhász, A., Luhmann, J.G., 1991. The dynamics of submicron-sized dust particles lost from Phobos. J. Geophys. Res. 96, 11,283–11,290.

Ishimoto, H., 1996. Formation of Phobos/Deimos dust rings. Icarus 122, 153–165.

Juhász, A., Horányi, M., 1995. Dust torus around Mars. J. Geophys. Res. 100, 3277–3284.

Krauss, O., Wurm, G., 2005. Photophoresis and the pile-up of dust in young circumstellar disks. Astrophys. J. 630, 1088–1092.

Krivov, A.V., 1994. On the dust belts of Mars. Astron. Astrophys. 291, 657–663.

Krivov, A.V., Hamilton, D.P., 1997. Martian dust belts: waiting for discovery. Icarus 128, 335–353.

Krivov, A.V., Jurewicz, A., 1999. The ethereal dust envelopes of the Martian moons. Planet. Space Sci. 47, 45–56.

Krivov, A.V., Sokolov, L.L., Dikarev, V.V., 1996. Dynamics of Mars-orbiting dust: effects of light pressure and planetary oblateness. Celestial Mech. Dyn. Astron. 63, 313–339.

Krivov, A.V., Krüger, H., Grün, E., Thiessenhusen, K., Hamilton, D.P., 2002. A tenuous dust ring of Jupiter formed by escaping ejecta from the Galilean satellites. J. Geophys. Res. 107, 10.1029/2000JE001434.

Krivov, A.V., Feofilov, A.G., Dikarev, V.V., 2006. Search for the putative dust belts of Mars: the late 2007 opportunity. Planet. Space Sci., this issue.

Landau, L.D., Lifshitz, E.M., 1965. Mechanics. Oxford University Press, Oxford.

Makuch, M., Krivov, A.V., Spahn, F., 2005. Long-term dynamical evolution of dusty ejecta from Deimos. Planet. Space Sci. 53, 357–369.

Mannella, R., 2000. A gentle introduction to the integration of stochastic differential equations. In: Freund, J.A., Pöschel, T. (Eds.), Stochastic Processes in Physics, Chemistry, and Biology. Springer, Dordrecht, pp. 353–364.

Mannella, R., Palleschi, V., 1989. Fast and precise algorithm for computer simulation of stochastic differential equations. Phys. Rev. A 40, 3381–3386.

Milstein, G.N., Repin, Yu.M., Tretyakov, M.V., 2002. Symplectic integration of Hamiltonian systems with additive noise. SIAM J. Numer. Anal. 39, 2066–2088.

Pierre, A.G.S., Steele, W.A., 1969. Time correlations and conditional distribution functions for classical ensembles of free rotors. Phys. Rev. 184 (1), 172–186.

Purcell, E.M., 1979. Suprathermal rotation of interstellar grains. Astrophys. J. 231, 404–416.

Resibois, P., de Leener, M., 1977. Classical Kinetic Theory of Fluids. Wiley, New York.

Roatsch, T. (Ed.), 1988. Data of the Planetary System. Akademie-Verlag, Berlin.

Skoglov, E., 2002. The influence of the spin vectors of asteroids from the Yarkovsky effect. Astron. Astrophys. 393, 673–683.

Spahn, F., Krivov, A.V., Sremčević, M., Schwarz, U., Kurths, J., 2003. Stochastic forces in circumplanetary dust dynamics. J. Geophys. Res. 108, 5021, doi:10.1029/2002JE001925.

Spitale, J., Greenberg, R., 2001. Numerical evaluation of the general Yarkovsky effect: effects on semimajor axis. Icarus 149, 222–234.

Vokrouhlicky, D., Capek, D., 2002. Yorp-induced long-term evolution of the spin state of small asteroids and meteoroids: Rubincam's approximation. Icarus 159, 449–467.